Influence of hollow-core wall panels on the cyclic behavior of different types of steel framing systems

Parsa Monfaredi, Mehdi Nazarpour, and Abdoreza S. Moghadam

- This paper presents the results of an experimental program that evaluated the seismic behavior of steel frames with hollow-core wall panels under reversed cyclic loading and discusses the effects of the hollow-core panels.
- Three half-scale, single-story, single-bay steel frames were built and tested. One test specimen was a bare moment frame with a rigid connection frame, and the other two had hollow-core wall panels. Of the two hollow-core specimens, one had a rigid connection and the other had a pinned connection frame.
- The test results indicated that hollow-core panels within the frame could provide additional stiffness and strength and have a positive impact on the overall seismic response of the structure.

PCI Journal (ISSN 0887-9672) V. 66, No. 5, September–October 2021.
PCI Journal is published bimonthly by the Precast/Prestressed Concrete Institute, 8770 W. Bryn Mawr Ave., Suite 1150, Chicago, IL 60631.

Precast concrete hollow-core panels are common components in modern buildings. Because of ease and time savings with installation and finish, they are useful in residential, commercial, warehouse, and industrial buildings as exterior or interior partitions. In addition, hollow-core panels are used as nonstructural components in lateral-load-bearing systems.

Only a few studies have evaluated the seismic performance of hollow-core wall panels. For example, Hamid and Ghani[1] carried out an experimental study on seismic behavior of hollow-core walls under biaxial lateral cyclic loading. In their study, two wall specimens were detailed with steel armoring at the base-to-foundation interfaces, including supplementary unbonded post-tensioned prestress, fuse bars, and mechanical energy dissipators. Bora et al.[2] used a slotted-bolted friction joint to avoid brittle wall or anchorage failure in thin hollow-core precast concrete panels. Holden et al.[3] discussed the armoring details based on rocking behavior. Perez et al.[4] introduced the seismic design requirements for precast concrete walls with additional details such as shear connectors and spiral reinforcement.

Previous studies have demonstrated that single hollow-core walls are capable of resisting substantial lateral loads, despite their lack of transverse shear reinforcement, if connection details are modified.[5] There is a significant uncertainty regarding the behavior of hollow-core wall panels under lateral loading without any modification to the connection details,[6] and further research has been needed to investigate

the effect of these panels on lateral load capacity, failure modes, and the energy dissipation capacity of the steel frame.

The aims of this study were to evaluate how hollow-core wall panels behaved in steel frames and present experimental results that could lead to the effective recognition of hollow-core wall behavior under cyclic lateral loading.

Research significance

Despite the findings of the previous studies, a firm conclusion cannot be drawn regarding the influence of hollow-core panels on the seismic performance of steel frames. The behavior of the infill walls is associated with several factors, including the rigidity of the beam-to-column connection. In particular, in gravity frames, the hollow-core panels have unidentified response to lateral loading that had not been examined in the literature.

To investigate the in-plane behavior of steel frames with rigid or even pinned connections of beams to columns, three identical half-scale steel frames were built and tested in the same manner. To examine the influence of inclusion of hollow-core panels, the steel moment-resisting frame and the gravity frame infilled with panels were compared with a frame with no infill walls. This study offers experimental results focused on overall response, modes of failure, energy dissipation, and stiffness-degrading behavior of the frames. The results of this study can be used in modifying and redesigning the hollow-core walls so that they can be considered the structural walls in regions with moderate to high seismic activity.

Experimental program

Specimens

Three identical half-scale, single-story, single-bay steel frames were designed and built in a laboratory setting. One assembly was a bare moment frame, while the others had wall units. All specimens were 1974 mm (77.7 in.) long × 1446 mm (56.9 in.) high. Infill panels consisted of 1260 × 880 × 150 mm (49.6 × 34.6 × 5.9 in.) hollow-core panels within a surrounding moment-resistant steel frame. **Figure 1** illustrates the geometry and dimensions of the test specimens, and **Table 1** summarizes the characteristics of the specimens.

Each specimen was defined by the type of frame and type of connection:

- Bare frame with rigid connection (BF-RC): Specimen BF-RC was the control, or reference, specimen and consisted of a bare frame with rigid reduced-beam-section connections.
- Vertical panels with rigid connection (VP-RC): Specimen VP-RC had two vertical, hollow-core panels in a rigid connection frame, or moment frame.
- Vertical panels with pinned connection (VP-PC): Specimen VP-PC had two vertical, hollow-core panels in a pinned connection frame, or gravity frame.

For specimen VP-RC and specimen VP-PC, the panels were separated from the steel column by 14 mm (0.55 in.) vertical gaps. Specimen VP-PC represents a single-bay infilled frame in a conventional steel frame with shear walls so that the beam-to-column connections were not rigid and the steel frame was assumed to resist only the gravity loads.

Hollow-core panels were manufactured with longitudinal cores and two layers of high-strength bonded pretensioning strands, filled with high-strength and very-low-slump concrete, and formed by extruders. Transverse reinforcement was not included. Box-section steel columns and built-up steel plate beams were constructed by a steel fabricator and then assembled into a frame with the hollow-core panels. Longitudinal fillet welds joined four steel plates to form the steel box columns (Fig. 1).

Materials

Standard test methods were used to determine the structural steel properties and the concrete compressive strength according to ASTM E8/E8M[7] and ASTM C39/C39M,[8] respectively.

Table 1. Summary of specimens

Specimen	Type of frame	Type of connection	Type of panels	Specimen dimensions, mm
BF-RC	Bare steel frame	Rigid	n/a	1974 × 1446
VP-RC	Steel moment frame with vertical panels	Rigid	Hollow-core with longitudinal cores and two layers of prestressed strands	1974 × 1446
VP-PC	Steel gravity frame with vertical panels	Pinned	Hollow-core with longitudinal cores and two layers of prestressed strands	1974 × 1446

Note: BF-RC = bare frame with rigid connection; n/a = not applicable; VP-PC = vertical panels in pinned connection frame; VP-RC = vertical panels in rigid connection frame. 1 mm = 0.0394 in.

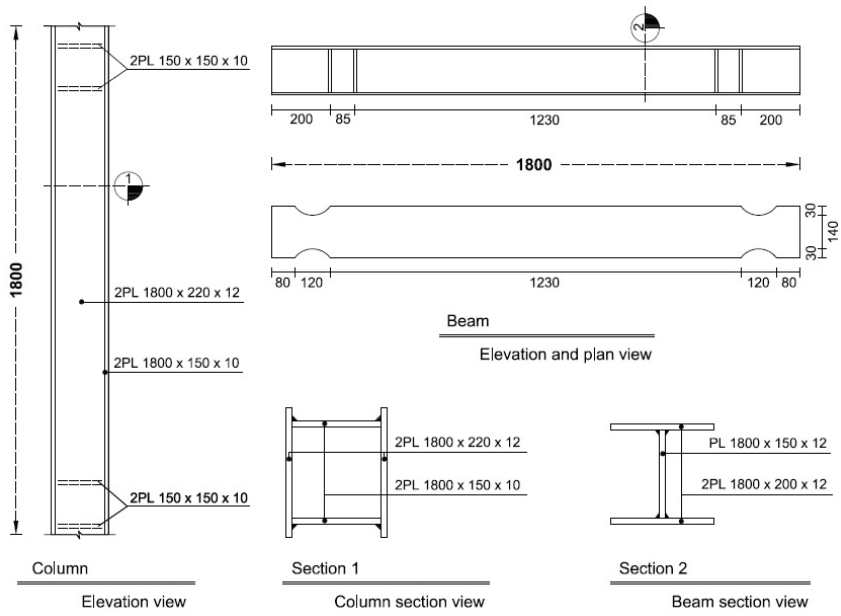

Beam and column details

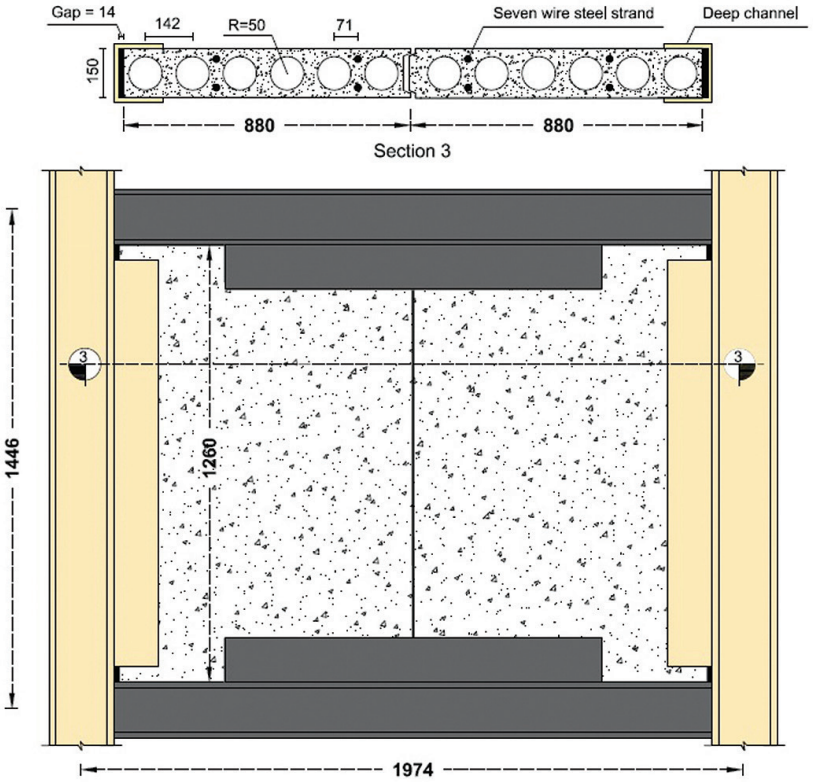

Specimen VP-RC and hollow-core wall section

Figure 1. Dimensions and geometry of test specimens. Note: All dimensions are in millimeters. PL = plate; R = radius; VP-RC = vertical panels in rigid connection frame. 1 mm = 0.0394 in.

ASTM A416/A416M[9] testing was performed on the strands. **Table 2** summarizes the material properties.

Test setup and instrumentation

Figure 2 shows the schematic arrangement of the experimental setup with an in-plane actuator attached to the reaction frame. Each column was fixed to the reaction frame by four anchored bolts. Lateral load was applied by a 1000 kN (225 kip) actuator, and the force was measured by an in-series load cell. Each specimen was loaded laterally with forces applied through the loading beam, which was a stiffened 220 mm (8.7 in.) deep European wide-flange beam IPB 220. A lateral force was applied at the center of the loading beam, which was located 1945 mm (76.6 in.) above the reaction frame.

Table 2. Material properties

Steel	Concrete	Strand
F_y = 293 MPa	f'_c = 58 MPa	Seven-wire steel strand
F_u = 420 MPa	w/c = 0.4	1860 MPa Grade LR ASTM A416
E = 205 GPa	Weight = 2403 kg/m³	Diameter = 8.35 mm

Note: E = modulus of elasticity of steel; f'_c = concrete compressive strength; F_u = ultimate tensile strength of steel; F_y = yield strength of steel; LR = low relaxation; w/c = water-cement ratio. 1 mm = 0.0394 in.; 1 MPa = 0.145 ksi; 1 GPa = 145 ksi; 1 kg/m³ = 1.6875 lb/yd³.

A constant low axial load was applied to the specimens by circular solid steel rods. The axial compression load in each column was 80 kN (18 kip). In addition, four 160 mm (6.3 in.) deep channels were attached to the beams and columns to prevent out-of-plane movement of the panels. To ensure that in-plane loading was imposed, lateral restraints were set up at the top corners of the specimens.

The experiments were conducted in drift control. In a displacement/drift control test, the displacement is the independent variable and the load reaction is the dependent variable. The drift ratio was calculated by dividing the difference between the displacements at the top and bottom of the steel moment frame by the column height. Two full cycles were applied at each target drift level during the test. Lateral displacements of the specimens were recorded with linear variable differential transformers and an image processing system that tracked the position of 70 points referred to as *markers*. The color pattern matching algorithm and the mean shift tracking algorithm were applied in image processing technique. All markers were placed on a 200 × 200 mm (7.9 × 7.9 in.) grid on the panels, columns, and beams.

The loading procedure was limited by the range of amplitude of the hydraulic actuator, which was 120 mm (4.7 in.) in both the positive direction (pulling) and the negative direction (pushing). Therefore, the applied displacements were the same for corresponding cycle numbers for all specimens, but the applied loads varied. In other words, loading tests were stopped at the maximum possible displacement of the hydraulic actuator, which corresponded to an ultimate drift ratio of 8.3%.

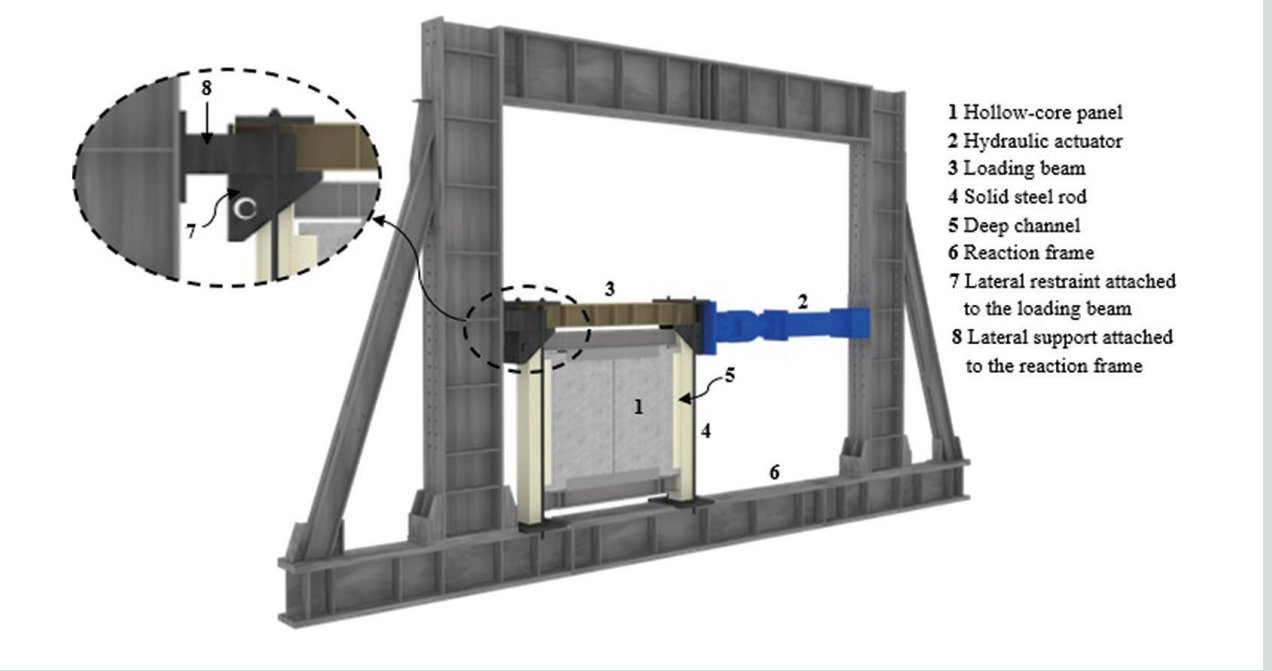

Figure 2. Illustration of the experimental setup showing specimen VP-RC. Note: VP-RC = vertical panels in rigid connection frame.

Loading history

All specimens were tested under quasi-static cyclic lateral loading. The in-plane lateral load was a series of displacement-controlled cycles in pull (positive displacement) and push (negative displacement) imposed by the actuator. The loading history is shown in **Fig 3**. Each complete load cycle consisted of one half cycle in each direction. This nominal loading history is similar to that specified by the Federal Emergency Management Agency's (FEMA's) *Interim Testing Protocols for Determining the Seismic Performance Characteristics of Structural and Nonstructural Components*.[10]

Test results and discussion

Overall response

Figure 4 plots the responses of specimens BF-RC, VP-RC, and VP-PC based on applied load versus drift ratio. **Table 3** summarizes the results. A comparison of load capacity showed that specimen VP-RC resisted higher loads than the other specimens; on average, its load capacity was 40% greater than that for specimen BF-RC in both directions (34% and 46% in the positive and negative direction, respectively). The peak load applied to specimen VP-PC exceeded the BF-RC specimen peak load by approximately 12%. From these results, we can conclude that the lateral load capacity of a frame is enhanced by hollow-core wall panels.

Figure 4 illustrates that hysteresis loops for frames with rigid connection exhibited less pinching than the conventional gravity frame with pinned connection. The pinching was most pronounced in specimen VP-PC due to the lack of a lateral-load-resisting system. Even though specimen BF-RC had more-stable and less-pinched hysteretic loops, its load-bearing capacity remained nearly constant after a drift ratio of 4%. A cyclic degradation of strength occurred in the frames with hollow-core panels such that the ultimate load was less than the peak load described in Table 3.

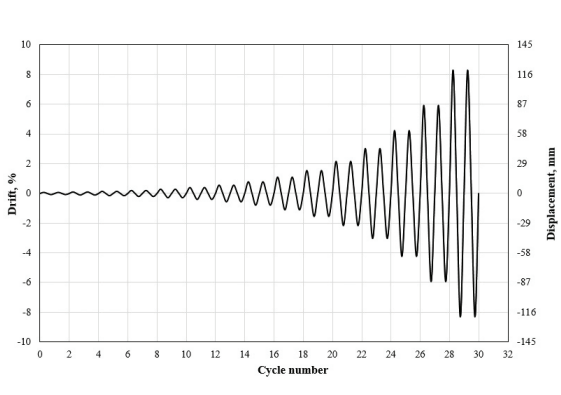

Figure 3. Loading history for each specimen in the experimental program. Note: 1 mm = 0.0394 in.

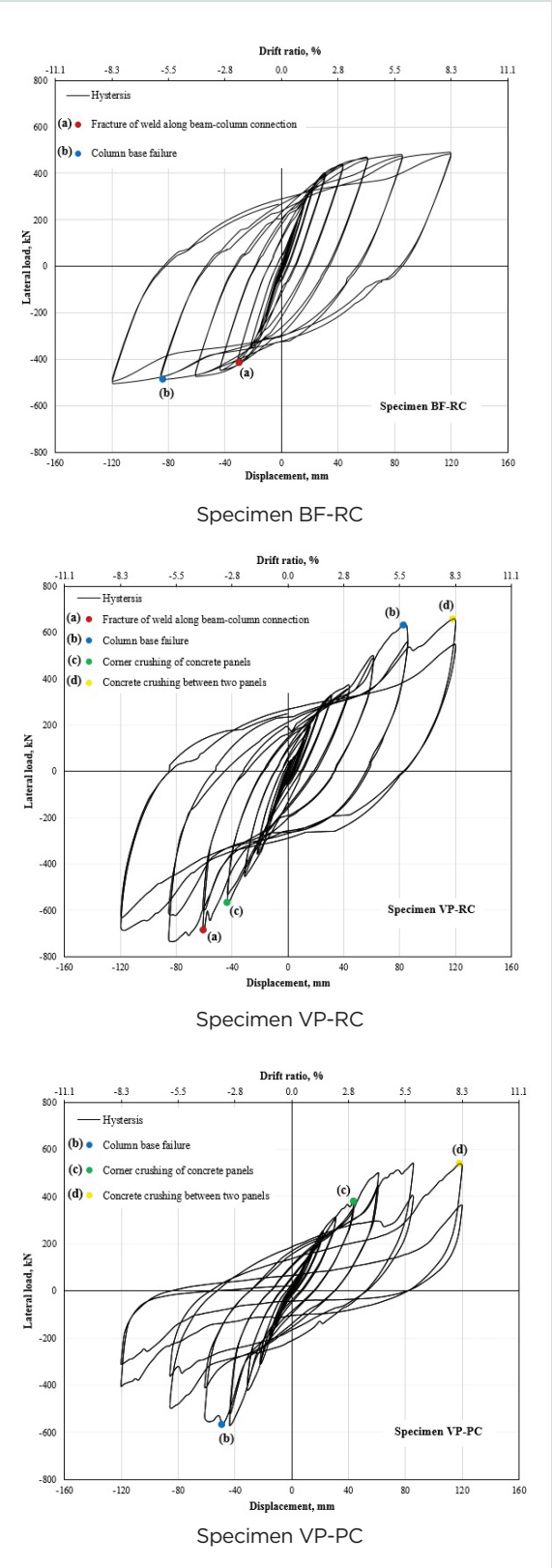

Figure 4. Experimental hysteresis curves. Note: BF-RC = bare frame with rigid connection; VP-RC = vertical panels in rigid connection frame; VP-PC = vertical panels in pinned connection frame. 1 mm = 0.0394 in.; 1 kN = 0.225 kip.

Table 3. Peak loads, ultimate loads, and measured drift ratios for each specimen

Specimen	Loading direction	Peak load, kN	δ_d, %	Ultimate load, kN	δ_u, %
BF-RC	+	491	8.3	491	8.3
	–	–503	–8.3	–503	–8.3
VP-RC	+	658	8.3	658	8.3
	–	–735	–5.9	–687	–8.3
VP-PC	+	542	5.9	538	8.3
	–	–572	–3.0	–406	–8.3

Note: BF-RC = bare frame with rigid connection; VP-PC = vertical panels in pinned connection frame; VP-RC = vertical panels in rigid connection frame; δ_d = drift ratio at peak load; δ_u =ultimate drift ratio at the last testing cycle. 1 kN = 0.225 kip.

The VP-RC specimen was able to maintain sufficient strength at large deformations (and therefore had high ductility) and resisted high loads at the ultimate drift ratio. The loading had to be stopped due to the limits of the hydraulic actuator stroke. Nevertheless, specimen VP-RC had a greater chance of additional load resistance compared with specimen BF-RC.

Modes of failure

Significant differences in the failure modes were observed between the bare frame and the infilled frames. In this regard, the types of damage were divided into two categories: damage to the structural components and damage to the nonstructural components, which are related to the steel frame and hollow-core panel, respectively. **Table 4** presents definitions of the failure modes and the corresponding loads and drift ratios.

Figure 5 illustrates the observed failure modes and damage for each specimen. The grid of markers for the image processing system can also be seen in Fig. 5. A comparison of the failure mechanisms revealed the advantage of hollow-core panels in the postponement of plastic hinge formation and reduction of damage severity in higher drift ratios. In relation to the failure of beam-to-column rigid connections, the peak load and corresponding drift ratio for specimen VP-RC were about 50% more than those for specimen BF-RC. As for the ultimate drift ratio, hollow-core panels in specimen VP-RC had severe damage, which led to a significant reduction of damage in its surrounding steel frame compared with the other specimens' steel frames.

Specimen VP-RC showed a rocking behavior under cyclic lateral loading (**Fig. 6**). In the final testing cycle, the maximum movements of the panels at the bottom corner were 15 and 95 mm (0.6 and 3.7 in.) in the horizontal and vertical directions, respectively; these values were determined using image processing techniques (Fig. 5). A similar behavior was observed in specimen VP-PC.

Corner crushing of concrete panels occurred due to the rocking behavior of the wall panels, which led to the high stress concentrations at each corner of the compression diagonal. As the drift ratio increased, corner crushing became more pronounced. Hollow-core panels of specimen VP-PC contributed to the load-bearing system from the beginning of loading. Consequently, compared with specimen VP-RC, compression struts in specimen VP-PC formed earlier and, in turn, corner crushing occurred in that specimen at a lower load.

As noted, specimen BF-RC failed in modes of structural

Table 4. Summary of failure modes, peak applied load, and drift ratio

Element	Sign	Failure mode	Specimen BF-RC		Specimen VP-RC		Specimen VP-PC	
			Load, kN	Drift ratio, %	Load, kN	Drift ratio, %	Load, kN	Drift ratio, %
Steel frame	(a)	Fracture of weld along beam-to-column connection	–412	–2.1	–686	–4.2	n/a	n/a
	(b)	Column base connection failure	–486	–5.8	633	5.7	–565	–3.4
Hollow-core wall panel	(c)	Corner crushing of concrete panels	n/a	n/a	–568	–3.0	379	3.0
	(d)	Concrete crushing between two panels	n/a	n/a	658	8.2	539	8.2

Note: BF-RC = bare frame with rigid connection; n/a = not applicable; VP-PC = vertical panels in pinned connection frame; VP-RC = vertical panels in rigid connection frame. 1 kN = 0.225 kip.

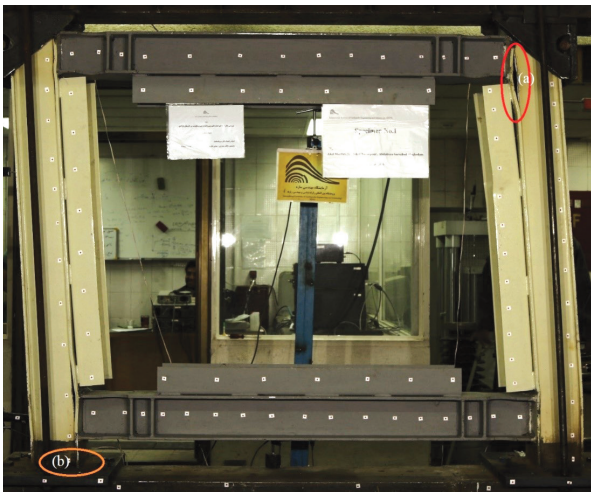

Specimen BF-RC

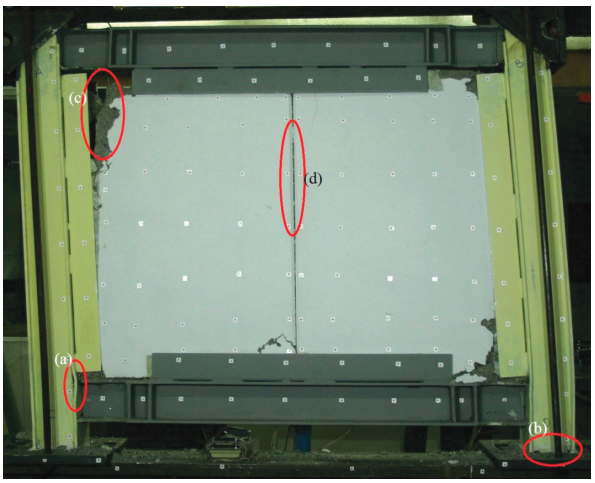

Specimen VP-RC

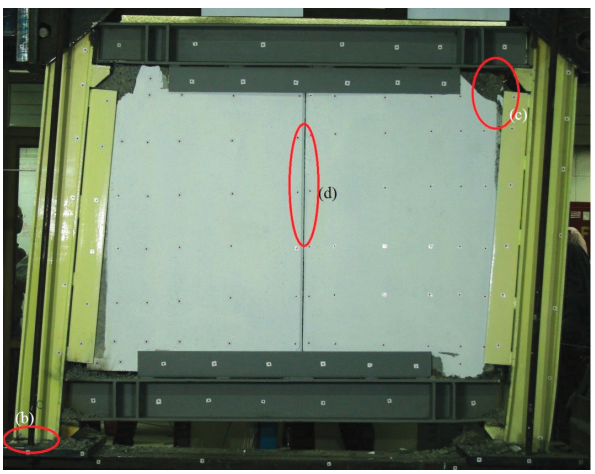

Specimen VP-PC

Figure 5. Observed failure modes and damage for specimen BF-RC, specimen VP-RC, and specimen VP-PC. Note: (a) = fracture of weld along beam-column connection; (b) = column base connection failure; BF-RC = bare frame with rigid connection; (c) = corner crushing of concrete panels; (d) = concrete crushing between two panels; VP-PC = vertical panels in pinned connection frame; VP-RC = vertical panels in rigid connection frame.

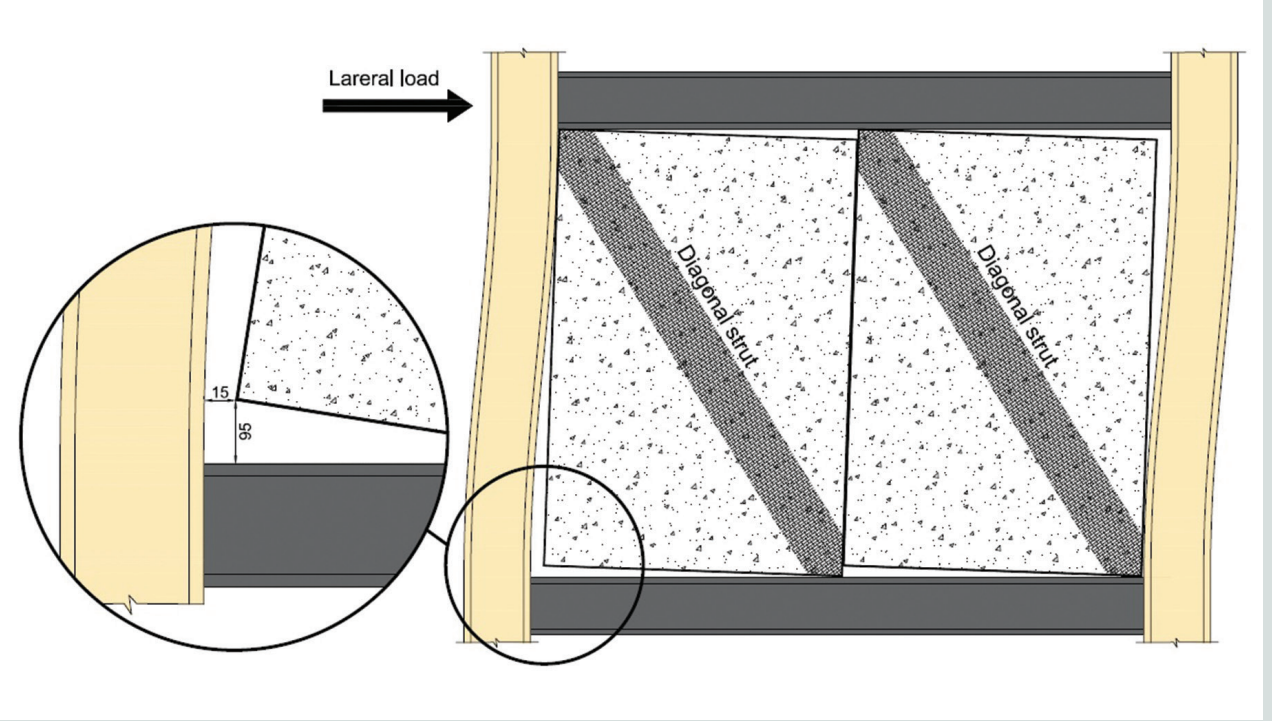

Figure 6. Rocking behavior of the VP-RC specimen at the ultimate drift ratio. Note: All dimensions are in millimeters. VP-RC = vertical panels in rigid connection frame. 1 mm = 0.0394 in.

components and experienced lower load capacity, whereas the identical frame with hollow-core panels (VP-RC) had panel-related failure modes and resulted in higher load-carrying capacity. This means that the hollow-core panels contributed to the reduction of the structural damage of the steel moment frame.

Backbone curve

Figure 7 shows the experimental backbone curves for the three specimens, which were derived from the American Society of Civil Engineers/Structural Engineering Institute (ASCE/SEI) 41-17, *Seismic Evaluation and Retrofit of Existing Buildings*,[11] and ASCE/SEI 41-06, *Seismic Rehabilitation of Existing Buildings*.[12] As specified in ASCE/SEI 41-17, the peak points of the first cycle at each displacement increment were connected to form the backbone curves, which are shown by solid black piecewise linear lines in Fig. 7. In FEMA guidance on the seismic rehabilitation of buildings[13,14] and ASCE/SEI 41-06, the backbone curve is drawn through the intersection of the first cycle curve for the deformation step *i* with the second cycle curve of the deformation step (*i*-1) for all steps *i*. The dashed lines are representative of the procedure proposed in ASCE/SEI 41-06.

There were differences in the values and trends of the two curves (Fig. 7). Regarding the trends, implementation of the procedures suggested by ASCE/SEI 41-06 led to the appearance of severe cyclic degradation of strength in the backbone curve of the VP-PC specimen. The differences between two cyclic backbone curves can be used as an indicator of brittleness: the greater the difference is, the more brittle the behavior will be. For example, specimen VP-PC showed a substantial difference (150%) between two backbone curves due to the behavior of the pinned connection and the severe damage to the column base.

Table 5 summarizes the values of the peak loads and the corresponding drift ratios obtained from both procedures. Specimen VP-PC showed the greatest difference in peak loads

Table 5. Peak load and corresponding drift ratio for the backbone curves

Specimen	Drift ratio, %	Peak load, kN		Difference, %
		ASCE/SEI 41-06	ASCE/SEI 41-17	
BF-RC	5.9	474	474	0
	–5.9	–463	–486	5
VP-RC	5.9	521	633	21
	–5.8	–538	–735	37
VP-PC	5.8	340	542	59
	–5.7	–199	–498	150

Note: ASCE = American Society of Civil Engineers; BF-RC = bare frame with rigid connection; SEI = Structural Engineering Institute; VP-PC = vertical panels in pinned connection frame; VP-RC = vertical panels in rigid connection frame. 1 kN = 0.225 kip.

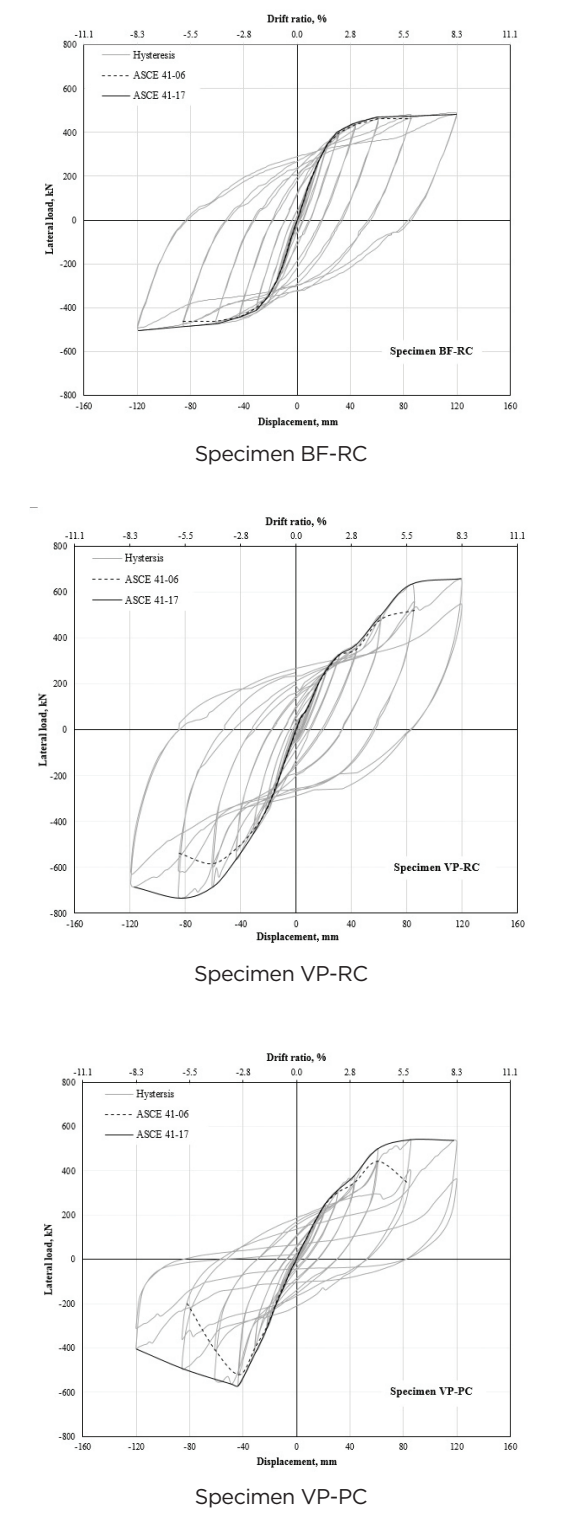

Figure 7. Cyclic backbone curves obtained from ASCE/SEI 41-17, *Seismic Evaluation and Retrofit of Existing Buildings*, and ASCE/SEI 41-06, *Seismic Rehabilitation of Existing Buildings*. Note: ASCE = American Society of Civil Engineers; BF-RC = bare frame with rigid connection; SEI = Structural Engineering Institute; VP-PC = vertical panels in pinned connection frame; VP-RC = vertical panels in rigid connection frame. 1 kN = 0.225 kip; 1 mm = 0.0394 in.

between the two backbone curves. Therefore, the behavior of specimen VP-PC was more brittle than the behavior of other specimens. In contrast, the backbone curves were almost the same in specimen BF-RC, so this specimen's behavior was less brittle than the behavior in the other specimens.

Figure 8 presents the backbone curves of the specimens derived from ASCE/SEI 41-17.[11] The maximum strength of specimen BF-RC was 66% and 89% of the maximum strengths of specimens VP-RC and VP-PC, respectively. Moreover, the strength of specimen VP-RC was up to 48% greater than the corresponding values in specimen VP-PC. The difference between the behaviors of specimens VP-RC and VP-PC was mainly attributed to the change in the connection's rigidity of the surrounding frames. In other words, pinned connections, not rigid connections, led to less contribution of infill in the steel frame.

Energy dissipation

The ability to dissipate energy is one of the important parameters for evaluating the seismic performance of structural walls. The energy dissipation is calculated on the basis of area enclosed by the load-displacement hysteresis loops. **Figure 9** illustrates the stacked value of energy dissipation capacity versus drift ratio.

At drift ratios less than or equal to 2.1%, the energy dissipation capacity of specimen VP-RC was similar to that of specimen BF-RC. This similarity is due to the gaps between panels and columns. Consequently, dissipating energy was limited by the moment frame. At drift ratios greater than 2.1%, gradual closing of the vertical gaps between panels

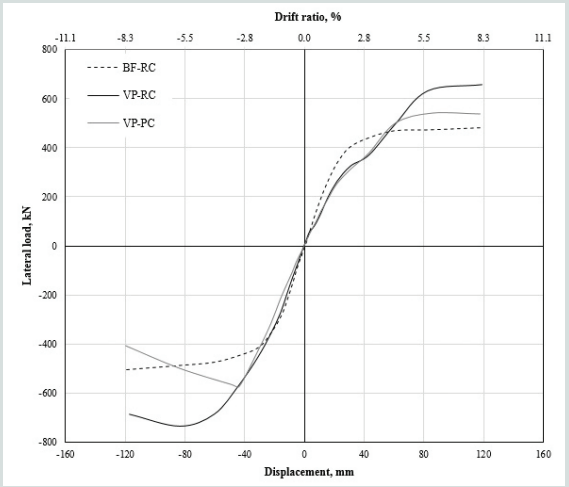

Figure 8. Comparison of the backbone curves obtained from ASCE/SEI 41-17, *Seismic Evaluation and Retrofit of Existing Buildings*. Note: ASCE = American Society of Civil Engineers; BF-RC = bare frame with rigid connection; SEI = Structural Engineering Institute; VP-PC = vertical panels in pinned connection frame; VP-RC = vertical panels in rigid connection frame. 1 kN = 0.225 kip; 1 mm = 0.0394 in.

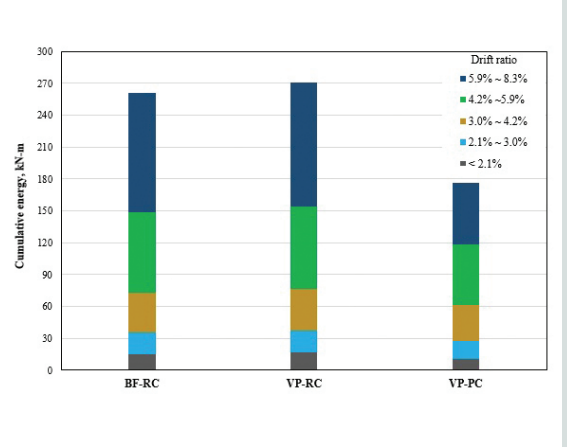

Figure 9. Relationship of the stacked value of cumulative energy-dissipation capacity to drift ratio. Note: BF-RC = bare frame with rigid connection; VP-PC = vertical panels in pinned connection frame; VP-RC = vertical panels in rigid connection frame. 1 kN-m = 8.85 kip-in.

and columns, formation of compression struts, and rocking behavior of hollow-core wall panels in specimen VP-RC caused a slight increase in energy dissipation comparison with specimen BF-RC.

The overall energy-dissipation capacity of the VP-RC specimen (270,745 kN-mm [2396 kip-in.]) was approximately 4% and 53% higher than the energy-dissipation capacities of specimens BF-RC and VP-PC, respectively (Fig. 9). For specimen VP-PC, the columns and hollow-core panels both participated in energy dissipation when the drift ratio range was between 2.1% and 5.9%. Subsequently, at drift ratios greater than 5.9%, the energy dissipation value remained constant due to severe damage to the specimen's column bases and panels. In fact, the frame was no longer able to dissipate energy and the main energy-dissipating element was the hollow-core panels.

For drift ratios less than or equal to 5.9%, the overall energy-dissipation capacity of the VP-PC specimen (118,605 kN-mm [1050 kip-in.]) was 20% less than that of specimen BF-RC and 23% less compared to specimen VP-PC. This finding demonstrates the considerable effects of the inclusion of hollow-core walls. As noted, the hollow-core panels contributed to the energy-dissipation mechanism in the gravity frame (VP-PC) and postponed the frame's main damages until the drift ratio exceeded 5.9%.

In conclusion, the presence of hollow-core panels increased the frames' energy-dissipating capability. These types of panels can act as dissipation devices, strongly reducing the damage in the structural elements, even though they are assumed to be nonstructural walls. Hence, hollow-core panels could help improve seismic behavior of the steel moment frame.

Stiffness-degrading behavior

Figure 10 plots the relationship of deduced values of cyclic stiffness to drift ratios. At the initial loading cycle, the hollow-core panels demonstrated no contribution in initial stiffness. Therefore, the initial stiffness values of specimens VP-RC and BF-RC were nearly the same (approximately 17 kN/mm [96.9 kip/in.]). By comparison, the initial stiffnesses of specimens VP-RC and BF-RC were 25% greater than that of specimen VP-PC.

At drift ratios equal to or less than 2.1%, the overall stiffness of the system was only associated with the steel frame members; this was an expected finding due to the gaps between panels and columns. Thus, for these drift ratios, the stiffness values of the VP-RC and BF-RC specimens exhibited the same pattern. At drift ratios greater than 2.1%, the gaps in specimen VP-RC gradually closed and ultimately led to stiffness that was 44% greater than the stiffness of specimen BF-RC. Because of the failure modes, gradual degradation in overall stiffness occurred in all specimens.

As for specimen VP-PC, because of the pinned connection, its initial stiffness was 20% less than that of the other specimens. The cyclic stiffness of specimen VP-PC was up to 11% greater than that of specimen BF-RC when the drift ratio was in the range of 3.5% to 7.0%, where failure of the column base connection in specimen VP-PC did not cause significant stiffness degradation. Clearly, the hollow-core panels were effective in preventing severe degradation of stiffness.

One of the major effects of hollow-core panels is a greater stiffness value compared with a bare frame when the drift ratio is between 2% and 8%. The greater stiffness value is due to the rocking behavior of the hollow-core panels and a better load transfer mechanism. Steel frames infilled with

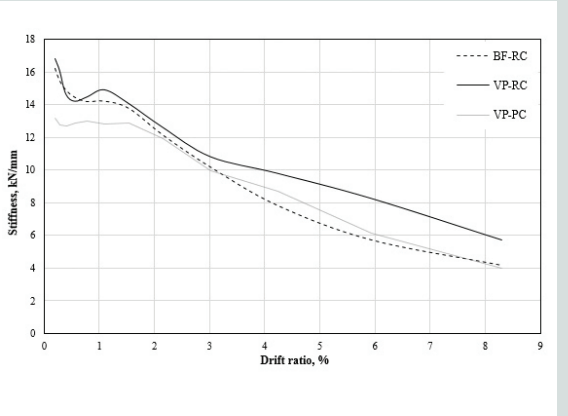

Figure 10. Relationship of cyclic stiffness response to drift ratio. Note: BF-RC = bare frame with rigid connection; VP-PC = vertical panels in pinned connection frame; VP-RC = vertical panels in rigid connection frame. 1 kN/mm = 5.71 kip/in.

hollow-core panels behave as a braced frame with the panels forming diagonal compression struts.

Less structural stiffness results in a longer natural period of vibration and, consequently, lower seismic force demand.[15] In contrast, greater initial stiffness causes more seismic force demand, which is undesirable. This is one of the reasons to have gaps between the infills and the structural elements. The gaps are to prevent the impact of the panels on the increment of initial stiffness. Following that, the same initial stiffness of both bare and infilled frames could be considered an advantage of these gaps.

Normalized dissipated energy

To compare the reduced energy dissipation per cycle in this study, the approach proposed by Kakaletsis and Karayannis was applied.[16] This approach had previously been used by researchers such as Tasnimi and Mohebkhah[17] and Emami and Mohammadi.[18] The energy-dissipation capacity per cycle was normalized by the peak-to-peak displacement 2Δ for that cycle, which was plotted against the imposed drift ratio (**Fig. 11**). 2Δ refers to the lateral displacement of the specimen in each complete cycle, which is in both directions. The distribution of plastic hinges in the steel frame and other damage to the system caused the dissipating energy to gradually increase. As a result, the normalized energy dissipation of the specimens increased as the drift ratio increased. The values of normalized energy dissipation of the BF-RC and VP-RC specimens were very similar when drift ratios were in the range of 1.0% to 5.0% (Fig. 11). However, after this stage, the normalized dissipated energy in specimen VP-RC was more than that of specimen BF-RC due to the presence of the infill panel in specimen VP-RC.

Although steel frames with pinned connections have low energy-dissipation capacity, specimen VP-PC experienced a significant amount of the normalized energy dissipation when the drift ratio was less than or equal to 5%. This improved behavior was caused by the inclusion of hollow-core panels. Finally, when the drift ratio was greater than 5%, the normalized dissipated energy of specimen VP-PC decreased due to severe damage in columns and panels.

Idealized backbone

Idealized backbone curves were obtained based on the proposed procedures of ASCE/SEI 41-17.[11] Because of the loading limitation of the hydraulic jack, which had a maximum displacement of 120 mm (4.7 in.) (target drift ratio of 8.3%), the experimental tests did not enter the degradation phase; therefore, the idealized curves are bilinear. **Figure 12** illustrates the bilinear idealization of the backbone response curve as a force-displacement relationship for the specimens. The first line segment of the idealized force displacement curve begins at the origin and has a slope equal to the effective lateral stiffness.

Table 6 presents the key parameters used to derive the idealized backbone curves. The effective lateral stiffness K_e, applied load at yielding V_y, applied load at ultimate strength V_d, lateral displacement at yielding Δ_y, lateral displacement at ultimate strength Δ_d, drift ratio at yielding δ_y, and drift ratio at ultimate strength δ_d are shown for both positive and negative loads. The effective (secant) stiffness was calculated as the slope of the line joining a yielding point on the idealized curve to the origin.

In comparison to the bare frame, the specimens with hollow-core panels experienced greater strength and stiffness capacity in the plastic range. This benefit of using hollow-core panels can improve the seismic performance level of the structure. As pointed out earlier, hollow-core walls did not contrib-

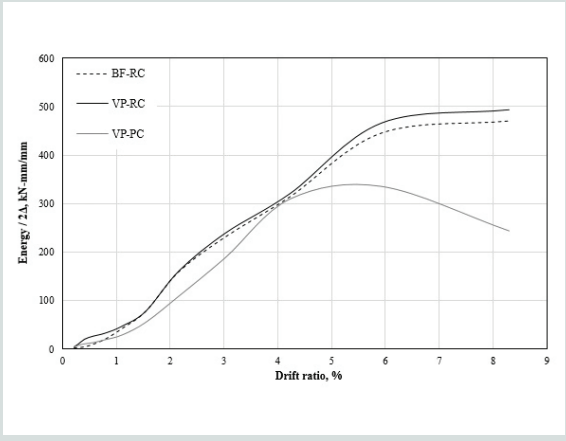

Figure 11. Comparison of the ratio of energy dissipation to displacement 2Δ per cycle against the drift ratio. Note: BF-RC = bare frame with rigid connection; VP-PC = vertical panels in pinned connection frame; VP-RC = vertical panels in rigid connection frame. 1 kN-mm/mm = 0.225 kip-in/in.

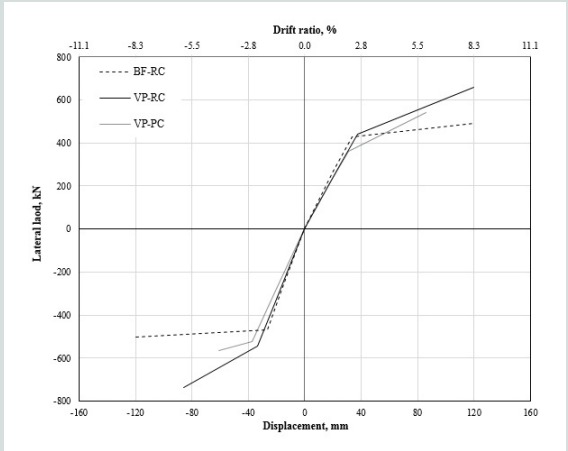

Figure 12. Idealized backbone curves. Note: BF-RC = bare frame with rigid connection; VP-PC = vertical panels in pinned connection frame; VP-RC = vertical panels in rigid connection frames. 1 mm = 0.0394 in.; 1 kN = 0.225 kip.

Table 6. Key parameters of each specimen for idealization backbone curves

Specimen	K_e, kN/mm	α_1	V_y, kN	V_d, kN	Δ_y, mm	Δ_d, mm	δ_y, mm	δ_d, mm
BF-RC	12.9	0.05	430	491	33.4	120	2.31	8.30
	–17.6	0.02	–469	–503	–26.6	–120	–1.84	–8.30
VP-RC	11.8	0.22	440	658	37.2	120	2.57	8.30
	–16.3	0.22	–545	–735	–33.4	–85.8	–2.31	–5.93
VP-PC	11.6	0.28	362	542	30.8	85.8	2.13	5.93
	–14.1	0.12	–523	–565	–37.2	–61.2	–2.57	–4.23

Note: BP-RC = bare frame with rigid connection; K_e = effective lateral stiffness of the specimen; V_d = applied load at ultimate strength; V_y = applied load at yielding; VP-PC = vertical panels in pinned connection frame; VP-RC = vertical panels in rigid connection frame; α_1 = positive post-yield slope ratio equal to the positive post-yield stiffness divided by the effective stiffness; δ_d = drift ratio at ultimate strength; δ_y = drift ratio at yielding; Δ_d = lateral displacement at ultimate strength; Δ_y = lateral displacement at yielding. 1 mm = 0.394 in.; 1 kN = 0.225 kip; 1 kN/mm = 5.71 kip/in.

ute to initial stiffness of the frame in the elastic range due to the gaps between panels and columns. Subsequently, the responses of the specimens were nearly identical up to yield. Therefore, the yielding point of both the VP-RC and VP-PC specimens were almost the same as the yielding point of specimen BF-RC. After this stage, the presence of hollow-core panels prevented the propagation of failures in the steel frame by rocking behavior. Thus, the slopes of second segments of idealized curves (post yield) of the VP-RC and VP-PC specimens were, respectively, about 4 and 5 times that of specimen BF-RC.

In order to highlight the advantages of hollow-core panels on the overall seismic behavior of steel frames, a comparison with conventional infills would be beneficial. Conventional infills, such as masonry infill walls, must be properly connected with the surrounding frame; however, the interaction between the infill wall and the frame may or may not be beneficial for the seismic behavior of the structure.[18] One of the disadvantages of this interaction is the greater initial stiffness of the frame, which leads to increased seismic demands. This may have an effect on the elastic behavior of the frame and change the yielding point area. This behavior of masonry-infilled frames in earthquake conditions was pointed out by Mohammadi and Emami.[19] In contrast, using hollow-core walls with a gap between panel and column resulted in an inconsequential change in the yielding point and improved plastic behavior of the frame.

It should be noted that the gap between the panel and column is one of the most effective parameters to improve structural performance levels; however, further research must be carried out to investigate the effective value of the gaps.

Conclusion

This paper described the effect of hollow-core infills on the cyclic behavior of both steel moment and gravity frames. The behavioral characteristics of the specimens were quantified with an emphasis on lateral load capacity, ductility, strength degradation attributes, hysteretic energy dissipation, and potential failure modes. The following conclusions were drawn from this investigation:

- The presence of hollow-core panels resulted in improved structural performance by transferring the failure events from the steel frame to the panels. This demonstrates that the panels are not, as they are often considered to be, nonstructural components.

- Separating panels from the steel column with 14 mm (0.55 in.) vertical gaps caused an identical initial stiffness of infilled and bare frames. One of the major effects of hollow-core panels was a greater stiffness value compared with the bare frame when the drift ratio was between 2% and 8%. The greater stiffness was caused by the panels' contribution to the load-bearing system, the rocking behavior of the hollow-core panels, and a better load transfer mechanism.

- The contribution of hollow-core panels in lateral load response of the steel frames when the drift ratio was greater than 2% led to a higher load-bearing capacity of the frames. Compared with specimen BF-RC, specimen VP-RC resisted loads up to 40% higher on average in both directions.

- Using hollow-core walls with a 14 mm (0.55 in.) gap between panel and column resulted in an inconsequential change in yielding point of the bare moment frame; a significant increment of the second line segment of the idealized backbone curve, which represents a positive post-yield slope ($\alpha_1 K_e$), increasing the lateral load capacity up to 46%; and overall improved plastic behavior of the frame.

- When the drift ratio was less than or equal to 2%, the steel frame was the main element of dissipating energy. When the drift ratio exceeded 2%, the effect of the frame on the dissipation energy mechanism decreased gradually as the drift ratio and frame damage increased, and the energy-dissipation contribution of the hollow-core panels increased. When the drift ratio was greater than 5.9%, the hollow-core walls exhibited a significant improvement in energy-dissipation capacity.

- The difference between the overall stiffness and strength of the infilled frame with pinned connection (specimen VP-PC) and the bare moment frame with rigid connections (specimen BF-RC) was not considerable. This finding demonstrates the significant effect that the type of connections has on stiffness and load-bearing capacity in steel frames. In summary, the stiffness and strength of the infilled frame with rigid connections (specimen VP-RC) were, respectively, up to 43% and 28% greater than the corresponding values in specimen VP-PC.

This experimental work determined that using hollow-core infills can enhance the seismic performance of steel frames subjected to the large deformations caused by severe earthquakes, despite the fact that they are regarded as nonstructural elements.

References

1. Hamid, N. H., and K. D. Ghani. 2013. "Seismic Behavior of a Precast Hollow Core Wall under Biaxial Lateral Cyclic Loading." *WIT Transactions on the Built Environment* 134: 815–825.

2. Bora, C., M. G. Oliva, S. D. Nakaki, and R. Becker. 2007. "Development of a Precast Concrete Shear-Wall System Requiring Special Code Acceptance." *PCI Journal* 52 (1): 122–135.

3. Holden, T., J. Restrepo, and J. B. Mander. 2003. "Seismic Performance of Precast Reinforced and Prestressed Concrete Walls." *Journal of Structural Engineering* 129 (3): 286–296.

4. Perez, F. J., S. Pessiki, and R. Sause. 2004. "Seismic Design of Unbonded Post-tensioned Precast Concrete Walls with Vertical Joint Connectors." *PCI Journal* 49 (1): 58–79.

5. Hamid, N. H. A., and J. B. Mander. 2006. "Experimental Study on Bi-lateral Seismic Performance of Precast Hollow Core Wall Using Shaking Table." In *Proceedings of the 10th East Asia-Pacific Conference on Structural Engineering and Construction (EASEC 2010)* (109–114). Bangkok, Thailand: Asian Institute of Technology.

6. Nazarpour, M., P. Monfaredi, and A. S. Moghadam. 2019. "Experimental Evaluation of Hollow-Core Wall Orientation in Steel Moment Frame." *PCI Journal* 64 (3): 92–103.

7. ASTM Subcommittee E28.04. 2009. *Standard Test Methods for Tension Testing of Metallic Materials*. ASTM E8/E8M-09. West Conshohocken, PA: ASTM International.

8. ASTM Subcommittee C09.61. 2001. *Standard Test Method for Compressive Strength of Cylindrical Concrete Specimens*. ASTM C39/C39M-01. West Conshohocken, PA: ASTM International.

9. ASTM Subcommittee A01.05. 2012. *Standard Specification for Steel Strand, Uncoated Seven-Wire for Prestressed Concrete*. ASTM A416/A416M-12. West Conshohocken, PA: ASTM International.

10. FEMA (Federal Emergency Management Agency). 2007. *Interim Testing Protocols for Determining the Seismic Performance Characteristics of Structural and Nonstructural Components*. FEMA 461. Washington, DC: FEMA.

11. ASCE (American Society of Civil Engineering)/SEI (Structural Engineering Institute). 2017. *Seismic Evaluation and Retrofit of Existing Buildings*. ASCE/SEI 41-17. Reston, VA: ASCE/SEI.

12. ASCE/SEI. 2007. *Seismic Rehabilitation of Existing Buildings*. ASCE/SEI 41-06. Reston, VA: ASCE/SEI.

13. FEMA. 1997. *NEHRP Guidelines for the Seismic Rehabilitation of Buildings*. FEMA 273. Washington, DC: FEMA.

14. FEMA. 2000. *Prestandard and Commentary for the Seismic Rehabilitation of Buildings*. FEMA 356. Washington, DC: FEMA. https://www.nehrp.gov/pdf/fema356.pdf.

15. Sharbatdar, M. K., and M. Saatcioglu. 2009. "Seismic Design of FRP Reinforced Concrete Structures." *Asian Journal of Applied Sciences* 2 (3): 211–222.

16. Kakaletsis, D. J., and C. G. Karayannis. 2008. "Influence of Masonry Strength and Openings on Infilled R/C Frames under Cycling Loading." *Journal of Earthquake Engineering* 12 (2): 197–221.

17. Tasnimi, A. A., and A. Mohebkhah. 2011. "Investigation on the Behavior of Brick-Infilled Steel Frames with Openings, Experimental and Analytical Approaches." *Engineering Structures* 33 (3): 968–980.

18. Emami, S. M. M., and M. Mohammadi. 2016. "Influence of Vertical Load on In-plane Behavior of Masonry Infilled Steel Frames." *Earthquakes and Structures* 11 (4): 609–627.

19. Mohammadi, M., and S. M. M. Emami. 2019. "Multi-bay and Pinned Connection Steel Infilled Frames; an Experimental and Numerical Study." *Engineering Structures* 188: 43–59.

Notation

E = modulus of elasticity of steel

f_c' = concrete compressive strength

F_u = ultimate tensile strength of steel

F_y = yield strength of steel

i = cycle number

K_e = effective lateral stiffness

V_d = applied load at ultimate strength

V_y = applied load at yielding

α_1 = positive post-yield slope ratio equal to the positive post-yield stiffness divided by the effective stiffness

δ_d = drift ratio at ultimate strength

δ_u = drift ratio at ultimate load

δ_y = drift ratio at yielding

Δ = lateral displacement in each half cycle

Δ_d = lateral displacement at ultimate strength

Δ_y = lateral displacement at yielding

About the authors

Parsa Monfaredi is a structural engineer in the Department of Structural Engineering at the International Institute of Earthquake Engineering and Seismology (IIEES) in Tehran, Iran, where he also received his MSc in the field of precast concrete hollow-core wall panels and steel structures.

Mehdi Nazarpour received his PhD from the IIEES Department of Structural Engineering in Tehran in 2019. The main fields of his research include precast concrete wall panels; high-strength concrete; squat reinforced concrete shear walls; and repair, rehabilitation, and retrofitting of structures.

Abdoreza S. Moghadam received his BS in civil engineering in 1987 and MS in structural engineering in 1991 from Tehran University and his PhD in earthquake engineering from McMaster University in Hamilton, ON, Canada, in 1999. His research interests include earthquake engineering, evaluation and design of tall buildings, development of building codes, seismic retrofitting of structures, and effects of three-dimensional modeling in building evaluation and design. He is currently an associate professor at IIEES in Tehran.

Abstract

Hollow-core precast concrete panels are widely used in commercial, industrial, and warehouse buildings as exterior or interior partitions. Because these infill walls are considered to be nonstructural elements, their interaction with the surrounding frame during an earthquake has been mostly neglected. This paper describes experimental research that evaluated the seismic behavior of different types of steel frames with hollow-core infill under reversed cyclic loading and discusses the effects of the hollow-core panels. Three identical half-scale steel frames were built and tested in the same manner. A steel moment-resisting frame and a gravity frame with hollow-core panels were compared with a frame with no infill walls. The test results indicated that under moderate to high shaking intensity, hollow-core panels rocked within the frame could provide additional stiffness, strength, and energy dissipation to the bare frame, as well as better flexibility and ductility. A comparison of failure mechanisms revealed the advantage of hollow-core panels in the postponement of plastic hinge formation and reduction of structural damage severity at higher drift ratios. This study shows that hollow-core walls can have a positive impact on the overall seismic response of the structure, despite the fact that they are regarded as nonstructural elements.

https://doi.org/10.15554/pcij66.5-02

Keywords

Failure mode, hollow-core, multipanel hollow-core wall, quasi-static cyclic loading, seismic behavior.

Review policy

This paper was reviewed in accordance with the Precast/Prestressed Concrete Institute's peer-review process.

Reader comments

Please address any reader comments to *PCI Journal* editor-in-chief Tom Klemens at tklemens@pci.org or Precast/Prestressed Concrete Institute, c/o *PCI Journal*, 8770 W. Bryn Mawr Ave., Suite 1150, Chicago, IL 60631.